Motional Dynamics of a Buried Tryptophan Reveals the Presence of Partially Structured Forms during Denaturation of Barstar

R. Swaminathan,[‡,§] Utpal Nath,[‖] Jayant B. Udgaonkar,*[,‖] N. Periasamy,*[,‡] and G. Krishnamoorthy*[,‡]

Chemical Physics Group, Tata Institute of Fundamental Research, Homi Bhabha Road, Bombay 400 005, India, and National Centre for Biological Sciences, TIFR Centre, P.O. Box 1234, Indian Institute of Science Campus, Bangalore 560 012, India

Received February 13, 1996; Revised Manuscript Received May 2, 1996[⊗]

ABSTRACT: A double mutant of the single-domain protein barstar having a single tryptophan (W53) was made by mutating the remaining two tryptophans (W38 and W44) into phenylalanines. W53 is buried in the core of barstar. Time-resolved fluorescence of the mutant barstar (W38FW44F) showed that W53 has a single fluorescence lifetime in the native (N) state and has three lifetimes in the molten globule-like low-pH (A) form. Quenching of fluorescence by either KI or acrylamide showed that W53 is solvent inaccessible in the N-state and fairly accessible in the A-form. The denaturation of W38FW44F by guanidine hydrochloride (GdnHCl) was monitored by several probes: near-UV and far-UV circular dichroism (CD), fluorescence intensity, and steady-state and time-resolved fluorescence anisotropy. While the unfolding transitions observed through CD and fluorescence intensity coincided with each other (midpoint $\approx$ 1.8 M GdnHCl), the transition observed through the steady-state fluorescence anisotropy was markedly different from others. Initially, the anisotropy increased with the increase in the concentration of GdnHCl and decreased subsequently. The midpoint of this titration was 2.2 M GdnHCl. Picosecond time-resolved fluorescence anisotropy showed that W38FW44F has a single rotational correlation time of 4.1 ns in the native (N) state and 1.5 ns in the unfolded (U) state (6 M GdnHCl). These could be explained as being due to the absence of motional freedom of W53 in the N-state and the presence of rotational freedom in the U-state. In the intermediate concentration region (1.8−3.0 M GdnHCl), the anisotropy decays showed at least two correlation times, $\sim$1 and 6−12 ns. These two correlation times are ascribed to partially structured forms leading to hindered rotation of W53. Thus, the usefulness of time-resolved fluorescence anisotropy in detecting partially folded structures is demonstrated.

Equilibrium unfolding of globular proteins by denaturants offers insights into the various interactions that govern the stability of protein structures and the pathway of protein folding. The process of unfolding by denaturants has often been modeled by a two-state mechanism involving the native (N) and the fully unfolded (U) forms (Privalov, 1992; Karplus & Shakhnovich, 1992). The nearly identical unfolding transitions observed by both the secondary structure probe (far-UV CD) and the tertiary structure probe (fluorescence intensity) have been generally taken as an indication for the two-state model in many situations [Khurana and Udgaonkar (1994) for example]. Although such observations by themselves cannot be taken as sufficient evidence for the two-state mechanism (see Discussion), the two-state model has been found to be very useful in evaluating the various factors that control the structural stability. These could be factors such as pH, temperature, ionic strength, etc. The use of site-directed mutagenesis in evaluating the various interactions that govern the structural stability also relies on the application of the two-state model. Such analyses are generally impractical using a multistep model due to the inherent difficulty in characterizing the intermediate (I) state(s).

The lack of appropriate probes is one of the likely reasons for the nonobservation of intermediate states in many cases. Detection of any partially folded structure under equilibrium conditions would offer significant insights into the mechanism of protein folding (Dill & Shortle, 1991; Ptitsyn, 1992; Nath & Udgaonkar, 1995; Doniach et al., 1995). Although the question whether partially folded structures (such as molten globule, for example) observed under equilibrium conditions are intermediates in the kinetic pathway of folding has not been answered in many systems [see, however, Vidugiris et al. (1995) and Ptitsyn et al. (1990)], their characterization is nevertheless useful.

In this paper, we report our observations on the motional dynamics of the single tryptophan (Trp53) side chain in the double mutant (W38FW44F)[1] of barstar using the time-resolved fluorescence technique. Barstar, which is a single-domain protein having four α-helices and a three-stranded parallel β-sheet (Guillet et al., 1993; Lubienski et al., 1994), is an attractive model for studying protein folding. Earlier studies on barstar have shown the existence of several kinetic intermediates (Shastry et al., 1994; Shastry & Udgaonkar, 1995; Agashe et al., 1995) and equilibrium intermediates

* Authors for correspondence.
‡ Tata Institute of Fundamental Research.
§ Present address: Cardiovascular Research Institute, 1246 Health Sciences East Tower, University of California, San Francisco, CA 94143-0521.
‖ National Centre for Biological Sciences.
⊗ Abstract published in *Advance ACS Abstracts,* June 15, 1996.

[1] Abbreviations: CD, circular dichroism; GdnHCl, guanidine hydrochloride; DTT, dithiothreitol; EDTA, ethylenediaminetetraacetic acid; trp, tryptophan; W38FW44F, the double mutant of barstar where the side chains Trp38 and Trp44 are mutated to phenylalanines; W53F, the single mutant of barstar where the side chain Trp53 is mutated to phenylalanine; N-state, native state at pH 7; A-form, molten globule-like acid form at pH 3; U-state, GdnHCl-denatured state; MEM, maximum entropy method; wt, wild type.

S0006-2960(96)00347-9 CCC: $12.00

such as molten globular (A) form at low pH values (Khurana & Udgaonkar, 1994; Swaminathan et al., 1994) and another intermediate form in a mutant barstar (Nath & Udgaonkar, 1995). W53 is located in the core of barstar. Hence the dynamic fluorescence measurements on W38FW44F are expected to offer insights into the nature of the core during the folding/unfolding transition. Since dynamic fluorescence measurements are more sensitive when compared to steady-state fluorescence (Eftink, 1994), they could be expected to indicate the presence of any intermediate(s) during the transition. In fact, the fluorescence anisotropy studies presented here do show the presence of structure(s) which are partially folded around Trp53.

MATERIALS AND METHODS

Chemicals. Chomatographic resins, GdnHCl, Torula yeast RNA, etc., were obtained from Sigma; SP-Trisacryl was from IBF, and dialysis tubes (molecular weight 3500 cutoff) were from Spectrum Medical Industries. *Taq* polymerase was from Boehringer Mannheim, and restriction enzymes were from New England Biolab. DNA sequencing was done using Sequenase Version 2.0 obtained from Amersham. All other chemicals were of analytical grade.

Bacterial Strains, Plasmids, and Site-Directed Mutagenesis. The *Escherichia coli* strain used for protein expression was MM294 *(supE44 hsdR endAl pro thi)*. The barnase and barstar expression plasmids, pMT416 and pMT316, respectively, were kindly provided by Dr. R. W. Hartley (1988). Oligonucleotide-directed mutagenesis was done by PCR, as described earlier (Merino et al., 1992; Nath & Udgaonkar, 1995). The mutagenic primers used to change W38 to F38 and W44 to F44 were G GAC GCT TTA TTC* GAT TGT CT and ACC GGA TT*T* GTG GAG TAC C. The three end primers were ACA CAG GAA ACA GGA TCC GT, AAG GCC TTG TCG ACC CCC ATT ACG GCA AGC TTG GGG, and AAG GCC TTG TCG ACC CCC. The mutations were verified by dideoxy sequencing (Sanger et al., 1977) of the entire mutant barstar gene.

Expression and Purification of Barstar and Barnase. The procedure for the purification of W38FW44F was similar to that described earlier for wt barstar (Khurana & Udgaonkar, 1994). The yield of the mutant was quite comparable to that of the wt protein (~200 mg/L *E. coli* growth). Barnase was purified as described by Paddon and Hartley (1987) and Mossakowska et al. (1989); the yield obtained was 8 mg/L.

The purity of each protein preparation was checked by SDS−PAGE (Schagger & Hagow, 1987). Barstar was found to be >98% pure, whereas the purity of barnase was >95%. Protein concentration was determined by a colorimetric assay (Bradford, 1976), and the extinction coefficients at 280 nm of wt barstar and W38FW44F were estimated to be 23 000 and 10 000 M^{-1} cm^{-1}, respectively. The activity of W38FW44F was about 100% of that of the wt barstar.

Fluorescence Measurements. Steady-state fluorescence measurements were carried out by using a SPEX Fluorolog FL1T11 T-format spectrofluorometer. Steady-state anisotropy was measured by monitoring the emission at parallel and perpendicular polarizations simultaneously by the use of the T-format optical arrangement. This method enhances the precision of measurement by removing the problems associated with sample instabilities.

Time-resolved fluorescence and anisotropy decay of barstar was measured by employing a CW mode-locked frequency-doubled Nd-YAG laser-driven dye (Rhodamine 6G) laser which generates 4−10 ps pulses. The protein was excited by using the second harmonic output (295 nm) of an angle-tuned KDP crystal. Fluorescence decay curves were obtained by using a time-correlated single photon counting setup coupled to a microchannel plate photomultiplier (Model 2809U; Hamamatsu Corp.). The instrument response function had a half-width of ~100 ps. Time-resolved anisotropy decays were analyzed on the basis of the model

$$I_{||}(t) = {}^1/_3 I(t)[1 + 2r(t)] \quad (1)$$

$$I_{\perp}(t) = {}^1/_3 I(t)[1 - r(t)] \quad (2)$$

$$I(t) = \sum_i \alpha_i \exp(-t/\tau_i) \quad i = 1-3 \quad (3)$$

$$r(t) = r_o \sum_j \beta_j \exp(-t/\tau_{r_j}) \quad j = 1 \text{ or } 2 \quad (4)$$

where $I_{||}$ and $I_{\perp}$ are the emission intensities collected at polarizations parallel or perpendicular to the polarization of the excitation beam. $I(t)$ is the total fluorescence intensity at time t. r_o is the initial anisotropy, and α_i and β_j are the amplitudes associated with the ith fluorescence lifetime and jth rotational correlation time such that $\Sigma\alpha_i = \Sigma\beta_j = 1$. In this model, each τ_i is associated with both τ_{r_1} and τ_{r_2}. $I_{||}$ and $I_{\perp}$ were analyzed globally (Swaminathan et al., 1994a). The accuracy of the estimated anisotropy decay parameters depended significantly on the accuracy of the geometry (G) factor of the emission monochromator. Hence, extreme care was taken in the estimation of the G-factor by using the laser dye BMQ dissolved in ethanol (lifetime of 0.83 ns and rotational correlation time of 0.2 ns). The steady-state fluorescence anisotropy (r_{ss}) was calculated from the parameters obtained from the time domain data by using

$$r_{ss} = \frac{r_o \sum_i \sum_j \alpha_i \beta_j (1/\tau_i + 1/\tau_{r_j})^{-1}}{\sum_i \alpha_i \tau_i} \quad (5)$$

Details of the instrument, the measurement techniques, and data analysis procedures are given elsewhere (Periasamy et al., 1988; Swaminathan et al., 1994a,b).

The average angular range of the hindered rotation of Trp53 was calculated by the model of isotropic diffusion inside a cone (Kinoshita et al., 1977). The semiangle Θ of the cone was calculated as

$$\Theta = \cos^{-1}\{{}^1/_2[[(1+8(\beta_2)^{1/2})^{1/2}] - 1]\} \quad (6)$$

CD measurements were carried out using a Jasco J720 spectropolarimeter. All the experiments were carried out at 23−25 °C. Experiments in the presence of denaturants were carried out during 1−3 h after the addition of the denaturant. Other details of the experimental methods are given in the figure legends.

Analysis of Steady-State Data. By assuming a two-state (N and U) model, we could write the steady-state fluorescence intensity (I_{ss}) and steady-state fluorescence anisotropy (r_{ss}) as

$$I_{ss} = \alpha_N \epsilon_N \phi_N + \alpha_U \epsilon_U \phi_U \quad (7)$$

$$r_{ss} = f_N r_N + f_U r_U \quad (8)$$

$$f_N = \alpha_N \epsilon_N \phi_N / (\alpha_N \epsilon_N \phi_N + \alpha_U \epsilon_U \phi_U) \quad (9)$$

with

$$\alpha_N + \alpha_U = f_N + f_U = 1 \quad (10)$$

α_N and α_U are the mole frations and f_N and f_U are the fractions of the emitted photons corresponding to the N- and U-states, respectively. ϵ and ϕ are the molar extinction coefficient and the fluorescence quantum yield, respectively. r_N and r_U are the anisotropy values corresponding to the N- and U-states, respectively. The fluorescence intensity data (Figure 1C) were fitted to eq 7 in order to get $\epsilon_N\phi_N$, $\epsilon_U\phi_U$, and the value of α_N at every concentration of GdnHCl. These values were then used to simulate r_{ss} by using eqs 8−10 and the values of r_N and r_U obtained at 0 and 5.7 M GdnHCl, respectively.

RESULTS

Steady-State Measurements. The stability of W38FW44F to denaturation by GdnHCl was identical to that of wt barstar when monitored through either CD or fluorescence intensity. Also, the activity of W38FW44F was nearly identical to that of wt barstar. Figure 1 shows the titration of various spectroscopic properties of W38FW44F with the denaturant GdnHCl. The titration of fluorescence intensity and CD (far- and near-UV) were nearly identical in their transitions. The midpoint of transition (1.8 M GdnHCl) obtained in these titrations is nearly identical to the observations with the wt barstar (Khurana & Udgaonkar, 1994). However, the steady-state fluorescence anisotropy (r_{ss}) showed a strikingly different behavior (Figure 1D). Firstly, r_{ss} showed a slight increase with the increase in the concentration of GdnHCl (in the range 0−1.5 M) and then decreased. Secondly, the midpoint of transition (∼2.2 M GdnHCl) was shifted to a higher value when compared to the other titrations (Figure 1A−C). These were observed consistently in a large number of repeated experiments. The difference in the midpoint of transition observed in the r_{ss} titration when compared to other titrations may be expected when one realizes that the scaling of r_{ss} with respect to concentrations is quite different from that of the scaling of other observables such as CD and fluorescence intensity (see eqs 7−10). The solid line in Figure 1D was simulated using eqs 7−10 and the fluorescence intensity data (Figure 1C) by assuming a two-state (N and U) model (see Materials and Methods). It can be clearly seen that the experimental values of r_{ss} do not agree with the simulation in the following two aspects: (i) the observed initial increase in r_{ss} cannot be fitted by the simulation and (ii) the observed midpoint of transition is still shifted by around 0.3 M GdnHCl when compared to the simulated curve.

Fluorescence Lifetime Measurements. The fluorescence decay of W38FW44F was found to follow a single exponential behavior ($\tau \sim 4.9$ ns) in the native (N) state (at pH 7) and a sum of three exponentials in the denatured (U) state and in the molten globular (A) form (at pH 3) (Figure 2 and Table 1). This behavior, especially the single-exponential decay in the N-state, was shown clearly in lifetime distribution also (Figure 3). This analysis, using the maximum entropy method (Skilling & Bryan, 1984; Livesey & Brochon, 1987; Swaminathan et al., 1994a,b), showed largely a

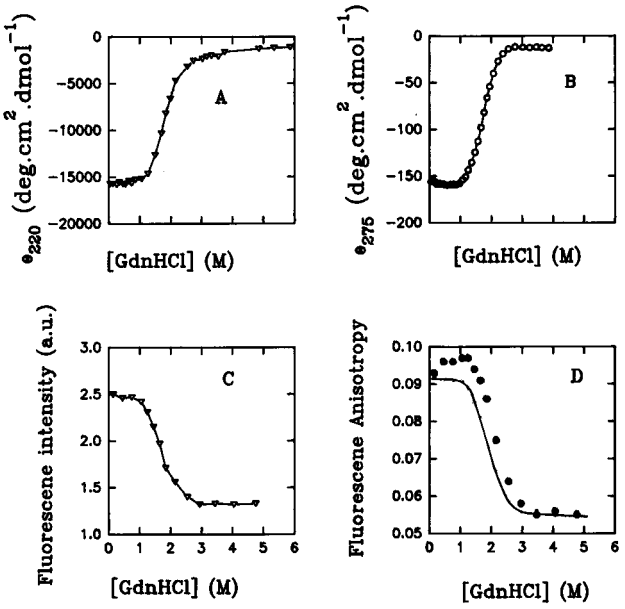

FIGURE 1: Titration of far-UV CD (A), near-UV CD (B), fluorescence intensity at 360 nm (excitation at 295 nm) (C), and steady-state fluorescence anisotropy at 360 nm (D) with GdnHCl. The concentration of W38FW44F was in the range of 10−100 μM in 20 mM phosphate, 1 mM EDTA, and 1 mM DTT at pH 7.0. The data represented are the average of 10−20 estimations. The uncertainty in the anisotropy values is less than 0.001. The midpoint of transitions was 1.8 M GdnHCl for far-UV CD (A), 1.75 M GdnHCl for near-UV CD (B) and fluorescence intensity (C), and 2.2 M GdnHCl for fluorescence anisotropy (D). The solid line in Figure 1D was simulated using eqs 7−10 and the data shown in Figure 1C (see text).

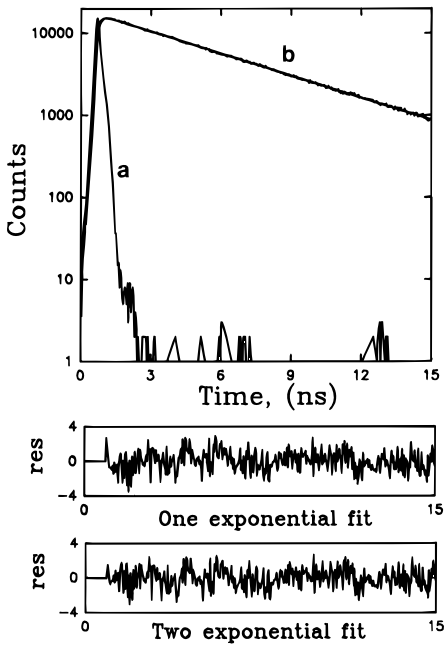

FIGURE 2: Fluorescence intensity decay of W38FW44F at pH 7. The excitation and emission wavelengths were 295 and 360 nm, respectively. The concentration of W38FW44F was 100 μm in 10 mM NaH_2PO_4 and 1 mM EDTA at pH 7.0. The excitation profile (a), emission profile (b), and calculated emission profile (smooth line in b) are shown. The time resolution was 37.8 ps per channel. The residual distribution for a one-exponential fit [$\tau = 4.82$ ns, $X^2 = 1.24$) and two exponential fit ($\tau_1 = 1.27$ ns (3%) and $\tau_2 = 4.84$ ns (97%), $X^2 = 1.18$] are also shown.

Table 1: Parameters Associated with the Decay of Fluorescence Intensity of W38FW44F

	conditions		fluorescence lifetimes[a] (ns)			amplitudes			
	pH	[GdnHCl] (M)	τ_1	τ_2	τ_3	α_1	α_2	α_3	mean lifetime[b] (ns)
1	3	0 (A-form)	5.25	2.12	0.53	0.25	0.43	0.32	2.39
2	7	0 (N-state)	4.90	–	–	1.0	–	–	4.90
3	7	0.3	4.89	–	–	1.0	–	–	4.89
4	7	0.8	4.90	3.50	0.22	0.86	0.08	0.06	4.50
5	7	1.1	4.95	3.40	0.22	0.77	0.11	0.12	4.21
6	7	1.5	5.28	3.47	0.23	0.46	0.38	0.17	3.75
7	7	1.7	5.16	3.06	0.24	0.48	0.37	0.15	3.65
8	7	1.9	5.06	2.64	0.25	0.40	0.37	0.23	3.06
9	7	2.2	4.71	2.24	0.39	0.32	0.44	0.24	2.57
10	7	2.6	4.49	2.14	0.34	0.21	0.51	0.29	2.12
11	7	3.5	4.01	1.95	0.33	0.26	0.48	0.26	2.06
12	7	4.2	3.99	1.97	0.36	0.26	0.48	0.26	2.06
13	7	5.7 (U-state)	3.98	2.02	0.38	0.28	0.47	0.25	2.16

[a] The errors in the values of τ_1 and τ_2 are less than 5%, and the error in the value of τ_3 is less than 20%. The value of the reduced chi square was in the range of 1.0−1.25 for all these data. [b] Mean lifetime $= \Sigma_i \alpha_i \tau_i$.

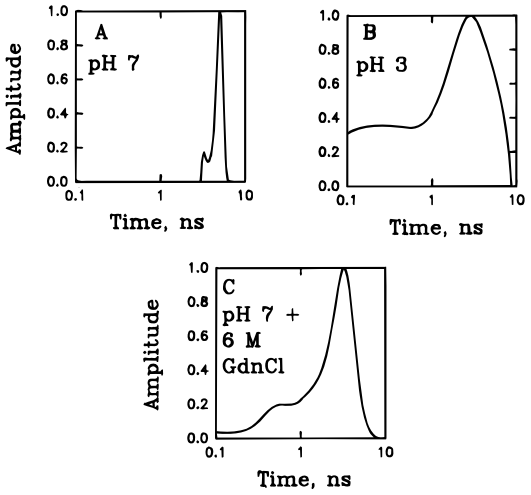

FIGURE 3: Fluorescence lifetime distributions obtained using MEM for W38FW44F at pH 7 (N-state), pH 7 with 6 M GdnHCl (U-state), and pH 3, (A-form). For the sample at pH 3 the solution had 10 mM glycine. Other experimental conditions are similar to those given in the legand to Figure 2.

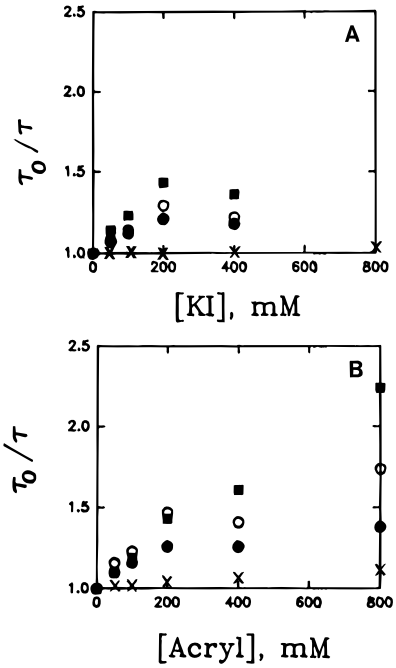

FIGURE 4: Stern−Volmer plots for the quenching of fluorescence lifetime(s) of W38FW44F in the N-state (pH 7) and in the A-form (pH 3), by either KI (A) or acrylamide (B). τ_o and τ are the lifetimes in the absence and in the presence of quencher, respectively: (×) pH 7 (N-state); (■) pH 3, mean lifetime; (○) pH 3, 2.1 ns component; (●) pH 3, 5.2 ns component. In the case of quenching by KI, the medium also contained $Na_2S_2O_3$ (100 μM) to avoid the formation of I_3^-. Other conditions are similar to those given in Figure 2.

narrow single peak in the N-state (Figure 3A), in stark contrast to our earlier observations on a number of single tryptophan proteins (Swaminathan et al., 1994b) (the minor second peak observed at ∼1.5 ns was about 3% of the total amplitude). The distribution obtained either in the U-state or in the A-form was significantly broader when compared to the distribution in the N-state.

The dependence of the fluorescence intensity decay kinetics with the concentration of GdnHCl is also given in Table 1. The decays followed a sum of three exponentials in all these cases. Two points are worthy of observation here. (i) The mean lifetime ($\tau_m = \Sigma \alpha_i \tau_i$) decreased monotonically with the increase in the concentration of GdnHCl, and the midpoint of titration (∼1.8 M) was similar to the midpoint observed in the titration of fluorescence intensity (Figure 1C). (ii) The value of the longest lifetime increased (from 4.9 to 5.3 ns) initially and decreased at higher (>2 M) concentrations of GdnHCl.

The solvent accessibility of Trp53 was checked by the quenching of fluorescence by either KI or acrylamide. Figure 4 shows the Stern−Volmer plots in the cases of the N-state and the A-form. It can be seen that Trp53 is almost inaccessible in the N-state (as shown by the insensitivity of the lifetime toward quenchers) and fairly accessible in the A-form (as shown by a significant decrease in the lifetime caused by either KI or acrylamide). Similar results were obtained when the steady-state fluorescence intensity was monitored instead of the lifetime (data not shown).

Time-Resolved Fluorescence Anisotropy Measurements. The steady-state anisotropy (r_{ss}) is a function of both the rotational dynamics of the fluorophore and its excited-state lifetime (eq 5). Hence, the variation in r_{ss} (Figure 1D) may not reflect the variation in the rotational dynamics alone. Hence, time-resolved fluorescence anisotropy decay was measured in order to get specific information on the rotational dynamics which could be related to the level of structural compactness around Trp53.

Fluorescence anisotropy decays were measured at various concentrations of GdnHCl (data not shown). There are

Table 2: Parameters Associated with the Decay of Fluorescence Anisotropy of W38FW44F at pH 7.0

	[GdnHCl] (M)	initial anisotropy r_o	rotational correlation times (ns)[a] τ_{r_1}	τ_{r_2}	amplitudes β_1	β_2	cone angle Θ (deg)	steady-state anisotropy[b] r_{ss}	X_{red}^2
1	0	0.20	−	4.1	0.0	1.0	0	0.091	1.38
2	0.3	0.20	−	4.1	0.0	1.0	0	0.091	1.54
3	0.8	0.20	−	4.0	0.0	1.0	0	0.094	1.60
4	1.5	0.19	−	4.8	0.0	1.0	0	0.107	1.41
5	1.7	0.19	0.93	5.7	0.06	0.94	12	0.093	1.40
6	1.9	0.19	1.02	6.2	0.17	0.83	20	0.090	1.23
7	2.2	0.18	1.47	11.9	0.53	0.47	39	0.085	1.27
8	2.6	0.17	0.90	6.9	0.63	0.37	45	0.064	1.13
9	3.5	0.13	1.50	−	1.0	0.0	90	0.055	1.13
10	4.2	0.14	1.60	−	1.0	0.0	90	0.061	1.11
11	4.9	0.14	1.46	−	1.0	0.0	90	0.057	1.15
12	5.7	0.14	1.54	−	1.0	0.0	90	0.058	1.20

[a] The error in the values of τ_r is about 10%. [b] r_{ss} calculated from the parameters of the time-domain data using eq 5.

several ways by which one could attempt to analyze these decay curves. One of the ways is by assuming a two-state model, namely the N- and U-states. The decays observed at 0 and 5.7 M GdnHCl could represent the two states N and U, respectively. The anisotropy decays in these two cases correspond to single exponentials with rotational correlation times (τ_r) of 4.1 and 1.5 ns (Table 2). These values are similar to those observed in the wt barstar (Swaminathan et al., 1994a). Anisotropy decays observed in the intermediate concentrations of GdnHCl (especially 1.8−3 M GdnHCl) could not be fitted either to a single exponential or to a linear combination of the anisotropy and fluorescence parameters obtained at 0 and 5.7 M GdnHCl. This shows clearly the inadequacy of the two-state model in describing the denaturation process. Further analysis of the anisotropy decays in the transition region showed that they could be fitted to a sum of two exponentials of time constants of ∼1.0 ns and another in the range of 6−12 ns (Table 2). The relative contribution of the shorter correlation time (1.0 ns) showed an increase with the increase in the concentration of GdnHCl (Table 2). Further, the values of the steady-state anisotropy (r_{ss}) calculated (eq 5) using the fluorescence lifetimes and time-resolved anisotropy data (Table 2) agree with the steady-state measurements of r_{ss} (Figure 1D). Overall, we observed that the changes in the anisotropy decay were not monotonic while going from the native to the denatured state. In contrast to this behavior, the anisotropy decay in the wt barstar changed monotonically from 0 to 6 M GdnHCl (data not shown). This could be due to the masking effect provided by the fluorescence from the other two Trp side chains (Trp38 and Trp44).

DISCUSSION

Motional Dynamics of Trp53 in the N-State and the A-Form. The side chain Trp53 is buried in the core of barstar as shown by both the crystal structure (Guillet et al., 1993) and the solution (NMR) structure (Lubienski et al., 1994). Hence, its dynamics is expected to reflect the flexibility of the core of barstar. The significant decrease in the steady-state fluorescence intensity in the presence of 6 M GdnHCl (Figure 1C) and the near inaccessibility of Trp53 by either KI or acrylamide (Figure 4) attest to the buried nature of Trp53 in the native state.

The fluorescence decay of wild type barstar (which has three Trp side chains) showed two lifetimes of 4.1 and 1.5 ns in the native state (Swaminathan et al., 1994a). On the basis of quenching studies, it was proposed that the 4.1 ns decay component arises from two of the three Trp side chains and that one of these two side chains is buried. Thus, the present observation of a single lifetime of 4.9 ns for Trp53 which is buried confirms our earlier assignment based on quenching studies. The increase in the value of the long lifetime component from 4.1 ns in the wild type to 4.9 ns in the mutant is likely to be due to the presence of quenching of fluorescence of Trp53 by other Trp side chains (Trp38 and Trp44) in the wt.

The single-exponential decay of Trp53 in the native state (Figure 2) deserves comment. Single-exponential decay of a single Trp protein is quite an unusual phenomenon indeed. The fluorescence decays of a large number of single Trp proteins follow multiexponential behavior (Beechem & Brand, 1985; Tanaka & Mataga, 1992; Eftink et al., 1991; Bismuto et al., 1993; Kim et al., 1993, Swaminathan et al., 1994a,b and references cited therein) except in a very few cases (Waldman et al., 1987; Shen, 1993; Willaert et al., 1992).

Multiexponential decay of Trp fluorescence has been generally attributed to multiple conformations (rotamers) around the $C_\alpha-C_\beta$ bond of the Trp side chain (Chen et al., 1987, 1991), multiple microstates of the protein (Haris & Hudson, 1990), or multiple structures of the protein (Chabbert et al., 1992; Kim et al., 1993). Our recent work (Swaminathan et al., 1994b) on the lifetime distributions of single Trp proteins has strongly suggested that multiple-exponential decay arises due to the presence of various rotamers of the Trp side chain. In light of these, the observation of single-exponential decay (Figure 2) for the N-state would indicate either the presence of a single conformation of the Trp53 side chain or the presence of high barriers for interconversions between various conformations. In contrast, the fluorescence decay followed a sum of three exponentials (Figure 2 and Table 1) in the A-form, indicating the presence of all three rotamers. The straightforward explanation for these observations is the following. The environment of Trp53 (and hence the core of barstar) is very rigid and devoid of any segmental mobility in the N-state but is quite flexible and highly dynamic in the A-form. The rigidity of the core in the native state should be to a level such that the Trp53 side chain is frozen in one of the rotamers, resulting in a single exponential fluorescence decay.

The rigidity of the core in the N-state and its flexibility in the A-form are supported by the following observations also.

(i) Trp53 which is inaccessible to either KI or acrylamide in the N-state becomes accessible in the A-form. (ii) The Trp side chain does not have any rotational freedom in the N-state as shown by the rotational correlation time τ_r (4.1 ns, Table 2) which represents the tumbling of the entire protein molecule with a molecular mass of 10.1 kDa. The lower value of τ_r (~1.5 ns) seen in the A-form indicates a high level of flexibility of the Trp side chain. (iii) The level of expression of the W53F mutant is drastically low (Utpal Nath, personal communication), indicating tight packing around Trp53 and hence destabilization of the protein upon its replacement.

The high level of flexibility of the Trp53 side chain in the A-form is in general agreement with the description of molten golbules as dynamic and flexible entities (Ptitsyn, 1992). However, studies on bovine and human α-lactalbumins and on bovine carbonic anhydrase have suggested that Trp side chains are nearly as restricted in the molten globular state as in the native state (Dolgikh et al., 1985; Rodionova et al., 1989). This difference could be due to the differences in the position of the Trp side chains in the various proteins. In the case of barstar, Trp53 is located between an α-helix (α1) and a β-strand (β2) (Guillet et al 1993, Lubienski et al., 1994). Hence, the motional freedom of Trp53 in the A-form would indicate the absence of strong tertiary interactions between the two secondary structural elements, α1 and β2. The high level of solvent accessibility of Trp53 in the A-form (Figure 4) also indicates loose packing of α1 and β2 in the A-form.

Beyond the Two-State Model of Protein Denaturation. As mentioned in the introductory section, the two-state model of protein denaturation is mainly based on nonobservation of any intermediate state during the denaturation process in many cases. Although there are numerous theoretical justifications for the two-state model (Shakhnovich & Finkelstein, 1982, 1989; Ueda et al., 1975; Go & Abe, 1982; Bryngelson & Wolynes, 1987, 1990; Skolinck et al., 1990; Shakhnovich & Gutin, 1989), the two-state model is very surprising since proteins are highly inhomogeneous systems whose structures are similar to disordered solids rather than to crystals (Karplus & Shakhnovich, 1992). Strong support for the two-state model has usually been provided by the following two observations: (i) identical or nearly identical unfolding transitions monitored by various techniques such as UV absorbance, fluorescence intensity, circular dichroism, etc. (Kim & Baldwin, 1990; Privalov, 1992), and (ii) agreement between the van't Hoff enthalpy of unfolding (measured by temperature dependence of the equilibrium constant between N and U) and direct microcalorimetric measurements (Privalov & Gill, 1988).

However, it should be emphasized that coincidence of unfolding transitions observed by a variety of probes is only a necessary but *not* a sufficient criterion for a two-state model. In general., the observations listed above would imply one of the following possibilities. (i) There are no intermediate states. (ii) The populations of intermediates are too small to be detected. (iii) The various probes used are not capable of bringing out the information regarding the existence of an intermediate state. In fact, the commonly used probes, such as UV absorbance, fluorescence, circular dichroism, etc., do not have a specific signature for an intermediate state when compared to both the N- and U-states. Apart from this, the selection of a target region of the molecule for observation could also be a factor in the success of observation of the intermediate.

Trp53 as a Probe of the Partially Structured Form. In the present study, we have chosen Trp53 as the probe in the mutant barstar. Trp53 is in the core of the protein (Guillet et al., 1993; Lubienski et al., 1994). The present study has shown that it is motionally very restricted in the N-state. The midpoint of titration of the steady state fluorescence anisotropy was shifted by about 0.3 M GdnHCl relative to the titrations of other observables (Figure 1). Unlike the other observables, such as optical absorption, fluorescence intensity, CD, etc., fluorescence anisotropy is quite specific to the motional dynamics (and hence the structural characteristics) of the probe. The inadequacy of the two-state model in fitting the observed dependence of r_{ss} with the concentration of GdnHCl (Figure 1) clearly shows the presence of at least one equilibrium intermediate state. This inadequacy could be seen by (i) the observed initial increase in the value of r_{ss} and (ii)the shift of ~0.3 M in the midpoint of transition of the r_{ss} titration when compared to the simulation based on the two-state model (eqs 7−10). The inadequacy of the two-state model could be seen in the following other observables also: (i) the initial decrease in the value of Θ_{275} (Figure 1B) and (ii) the initial increase in the value of the fluorescence lifetime (τ_1) from 4.9 to 5.3 ns and the subsequent decrease (Table 1). It is interesting to note that, while the mean lifetime (or the total intensity) behaves monotonically during the titration, an individual lifetime component does not.

The structural features of the intermediate form emerge from the time-resolved anisotropy measurements. The single rotational correlation times (τ_r) of 4.1 and 1.5 ns obtained at 0 and 5.7 M GdnHCl, respectively (Table 2), would correspond to the N- and U-states, respectively. τ_r of 4.1 ns in the N-state would imply the absence of any motional freedom for Trp53 and would reflect the tumbling of the entire protein. The shorter value of τ_r (1.5 ns) observed in the U-state would correspond to relatively free rotation of Trp53. These interpretations are similar to those given in the case of wt barstar (Swaminathan et al., 1994a).

The initial anisotropy (r_o) observed in the anisotropy decays was in the range of 0.20−0.14 which is significantly smaller than the value (0.27−0.35) observed in the case of Trp in rigid environments (Valeur & Weber, 1977; Ruggiero et al., 1990; Eftink et al., 1991). This may indicate a very fast unresolved motion of Trp53 in the protein. It is also known that r_o of Trp is sensitive to the excitation wavelength due to the presence of two excited states (^1L_a and ^1L_b) of indole (Valeur & Weber, 1977). The observed decrease in the value of r_o from 0.20 to 0.14 with the increase in the concentration of GdnHCl could also be due to shifts in the absorption spectra of the two states.

Anisotropy decays observed in the folding transition region (1.8−3 M GdnHCl) give the most interesting information. Analysis showed that they could be fitted to a sum of two correlation times, τ_{r_1} (1−1.5 ns) and τ_{r_2} (6−12 ns). These observations could be explained as follows. The transition region is populated by molecules having partial structures. This would lead to restricted rotational freedom around Trp53. The short correlation time of 1.0−1.5 ns would be consistent with the rotational freedom of Trp53 in these partial structures. The restricted nature of this rotational freedom could be inferred from the value of β_1 (<1) which

implies incomplete decay of anisotropy due to restrictions (Table 2). The remaining part of anisotropy decays by the tumbling of the entire (partially structured) molecule with a τ_{r2} of 6−12 ns. The cone angles for the restricted rotation calculated (Kinoshita et al., 1977) using the values of β_2 show an increase with the increase in the concentration of GdnHCl (Table 2). This is consistent with a decrease in the restriction of motional freedom of Trp53 with the increase in the concentration of GdnHCl. In the U-state, there is no restriction (cone angle = 90°) and the rotational motion with the correlation time of 1.5 ns depolarizes the anisotropy completely.

One could visualize the following picture in the transition region; Trp53 is wrapped around by a partially structured chain which imposes restrictions to its free rotation. As the concentration of GdnHCl increases, the restriction eases, thus leading to an increase in amplitude (β_1) of the restricted rotation. The higher value (6−12 ns) of τ_{r_2} when compared to the τ_r value of the N-state (4.1 ns) would be consistent with the increase in the average dimension of the partially structured form relative to the N-state. Thus, this picture indicates a gradual transition from the N-state to the U-state rather than a cooperative two-state model.

The foregoing analysis of anisotropy decay curves in the transition region has considered only the partially structured forms and has assumed that the populations of N- and U-states are negligibly small. Inclusion of the N- and U-states also in the analysis would lead to a situation of too many parameters for fitting the decay curves and result in nonunique fits of the data. However, since the main stress of this work is to show the inadequacy of the two-state model, the present level of analysis could be considered adequate. Also, the fair level of agreement between the values of r_{ss} calculated from time-domain parameters (Table 2) and those directly observed in steady-state experiments (Figure 1D) validates the present analysis of anisotropy decay curves. Further analysis using a model having three (or more) populations would have to wait for considerable improvement in the present technology of data collection.

The observation of the long correlation time ($\tau_{r_2} \sim 6-12$ ns) in the transition region could also be explained as being due to the formation of aggregates. It could be argued that aggregates are likely to form when the structure is partially opened so that the exposed hydrophobic regions from different molecules interact with each other. However, we did not observe any indication for the formation of aggregates in the transition region as mentioned below. The titration of the elution profile of barstar in a FPLC column (Superdex-75) with GdnHCl did not show formation of aggregates under the conditions of our experiments (data not shown).

The working hypothesis regarding the partial structure observed in the transition region is as follows. The region around Trp53 retains the structure to a large extent. This segment (which probably forms the core in the N-state) is attached to the remaining part of the molecule which is in an extended conformation, leading to significant increase in the overall dimension of the molecule. The direct implication of this model is that such a structure could be an early intermediate in the kinetic pathway of folding of barstar.

It should be mentioned that the present observation of gradual transition in the denaturation titration is not without precedence in other systems. Dill and Shortle (1991) have proposed continuous change between the N- and U-states as a general model for protein denaturation. Also, NMR observations on some proteins during denaturant titrations have shown that changes in the outer parts of the molecule proceed before the unfolding of the hydrophobic core (Bradburg & King, 1969; Benz & Roberts, 1973). More recently, an intermediate state which expands continuously with increasing concentration of GdnHCl has been observed in the case of the heat shock protein Dnak (Polleros et al., 1993).

Finally, the present studies have demonstrated the use of fluorescence anisotropy in revealing the presence of intermediate structural forms even in situations where the commonly used probes such as CD and fluorescence intensity do not indicate their presence. The ability of Trp53 to pick up partially structured form in W38FW44F could be related to its specific location within the structure. In order to check this hypothesis and the "continuous change model" in other single-domain proteins, the time-resolved anisotropy of other Trp probes could be used. This work is in progress.

REFERENCES

Agashe, V. R., Shastry, M. C. R., & Udgaonkar, J. B. (1995) *Nature 377*, 754−757.

Benz, F. W., & Roberts, G. C. K. (1973) *FEBS Lett. 29*, 263−266.

Bismuto, E., Gratton, E., Sirangelo, I., & Irace, G. (1993) *Eur. J. Biochem. 218*, 213−219.

Bradburg, J. H.,& King, N. L. R. (1969) *Nature 223*, 1154−1156.

Bradford, M. M. (1976) *Anal. Biochem. 72*, 248−254.

Bryngelson, J. D., & Wolynes, P. G. (1987) *Proc. Natl. Acad. Sci. U.S.A. 84*, 7524−7528.

Bryngelson, J. D., & Wolynes, P. G. (1990) *Biopolymers 30*, 177−188.

Chabbert, M., Hillen, W., Hansen, D., Takahashi, M., & Bousquet, J.-A. (1992) *Biochemistry 31*, 1951−1960.

Chen, L. X.-Q., Longworth, J. W., & Fleming, G. R. (1987) *Biophys. J. 51*, 865−873.

Chen, R. F., Knutson, J. R., Ziffer, H., & Porter, D. (1991) *Biochemistry 30*, 5184−5195.

Dill, K. A., & Shortle, D. (1991) *Annu. Rev. Biochem. 60*, 795−825.

Dolgikh, D. A., Abaturov, L. V., Bolotina, I. A., Brazhnikov, E. V., Bychkova, V. E., Bushuev, V. N., Gilmanshin, R. I., Lebedev, Yu. O., Semisotnov, G. V., Tiktopulo, E. I., & Ptitsyn, O. B. (1985) *Eur. Biophys. J. 13*, 109−121.

Doniach, S., Bascle, J., Garel, T., & Orland, H. (1995) *J. Mol. Biol. 254*, 960−967.

Eftink, M. R. (1994) *Biophys. J. 66*, 482−501.

Eftink, M. R., Gryczynski, I., Wiczk, W., Laczko, G., & Lakowicz, J. R. (1991) *Biochemistry 30*, 8945−8953.

Go, N., & Abe, H. (1981) *Biopolymers 20*, 991−1011.

Guillet, V., Lapthorn, A., Hartley, R. W., & Mauguen, Y. (1993) *Structure 1*, 165−176.

Harris, D. L., & Hudson, B. S. (1990) *Biochemistry 29*, 5276−5285.

Hartley, R. W. (1988) *J. Mol. Biol. 202*, 913−915.

Karplus, M., & Shakhnovich, E. (1992) in *Protein Folding* (Creighton, T. E., Ed.) pp 127−195, W. H. Freeman & Co., New York.

Khurana, R., & Udgaonkar, J. B. (1994) *Biochemistry 33*, 106−115.

Kim, P. S., & Badwin, R. L. (1990) *Annu. Rev. Biochem. 59*, 631−660.

Kim, S.-J., Chowdhury, F. N., Younathan, W. S. E. S., Rosso, P. S., & Barkley, M. D. (1993) *Biophys. J. 65*, 215−226.

Kinoshita, K. J., Kawato, S., & Ikegami, A. (1977) *Biophys. J. 20*, 289−305.

Livesey, A. K., & Brochon, J. C. (1987) *Biophys. J. 52*, 693−706.

Lubienski, M. J., Bycroft, M., Freund, S. M. V., & Fersht, A. R. (1994) *Biochemistry 33*, 8866−8877.

Merino, E., Osuna, J., Bolivar, F., & Fersht, A. R. (1992) *BioTechniques 12*, 508−509.

Mossakowska, D. E., Nyberg, K., & Fersht, A. R. (1989) *Biochemistry 28*, 3843−3850.
Nath, U., & Udgaonkar, J. B. (1995) *Biochemistry 34*, 1702−1713.
Paddon, C. J., & Hartley, R. W. (1987) *Gene 53*, 11−19.
Palleros, D. R., Shi, L., Reid, K. L., & Fink, A. L. (1993) *Biochemistry 32*, 4314−4321.
Periasamy, N., Doraiswamy, S., Maiya, G. B., & Venkataraman, B. (1988) *J. Chem. Phys. 88*, 1638−1651.
Privalov, P. L. (1992) in *Protein Folding* (Creighton, T. E., Ed.) pp 83−126, W. H. Freeman & Co., New York.
Privalov, P. L., & Gill, S. J. (1988) *Adv. Protein Chem. 39*, 191−234.
Ptitsyn, O. B. (1992) in *Protein Folding* (Creighton, T. E., Ed.) pp 243−300, W. H. Freeman & Co., New York.
Ptitsyn, O. B., Pain, R. H., Semisotnov, G. V., Zerovnik, E., & Razgulyaev, O. I. (1990) *FEBS Lett. 262*, 20−24.
Rodionova, N. A., Semisotnov, G. V., Kutyshenko, V. P., Uverski, V. N., Bolitina, I. A., Bychkova, V. E., & Ptitsyn, O. B. (1989) *Mol. Biol. (Moscow) 23*, 683−692.
Ruggiero, A. J., Todd, D. C., & Fleming, G. R. (1990) *J. Am. Chem. Soc. 112*, 1003−1014.
Sanger, F., Nicklen, S., & Coulson, A. R. (1977) *Proc. Natl. Acad. Sci. U. S. A. 74*, 5463−5467.
Schaggar, H., & von Jagow, G. (1987) *Anal. Biochem. 166*, 368−379.
Shakhnovich, E. I., & Finkelstein, A. V. (1982) *Dokl. Acad. Nauk SSSR 243*, 1247.
Shakhnovich, E. I., & Finkelstein, A. V. (1989) *Biopolymers 28*, 1667−1680.
Shakhnovich, E. I., & Gutin, A. M. (1989) *Stud. Biophys. 132*, 47.
Shastry, M. C. R., & Udgaonkar, J. B. (1995) *J. Mol. Biol. 247*, 1013−1027.
Shastry, M. C. R., Agashe, V. R., & Udgaonkar, J. B. (1994) *Protein Sci. 3*, 1409−1417.
Shen, W. H. (1993) *Biochemistry 32*, 13925−13932.
Skilling, J., & Bryan, R. K. (1984) *Mon. Not. R. Astron. Soc. 211*, 111−124.
Skolinck, J., Kolinski, A., & Yaris, R. (1990) *Comments Mol. Cell Biophys. 6*, 223.
Steer, B. A., & Merrill, A. R. (1995) *Biochemistry 34*, 7225−7233.
Swaminathan, R., Periasamy, N., Udgaonkar, J. B., & Krishnamoorthy, G. (1994a) *J. Phys. Chem. 98*, 9270−9278.
Swaminathan, R., Krishnamoorthy, G., & Periasamy, N. (1994b) *Biophys. J. 67*, 2013−2023.
Tanaka, F., & Mataga, N. (1992) in *Dynamics and Mechanisms of Photoinduced Transfer and Related Phenomena* (Mataga, N., Okada, T., & Masuhara, H., Eds.) pp 501−512, Elsevier Science Publishers, New York.
Ueda, Y., Taketomi, H., & Go, N. (1975) *Int. J. Pept. Protein Res. 7*, 445.
Valeur, B., & Weber, G. (1977) *Photochem. Photobiol. 25*, 441−444.
Vidugiris, G. J. A., Markley, J. L., & Royer, C. A. (1995) *Biochemistry 34*, 4909−4912.
Waldman, A. D. B., Clarke, A. R., Wigley, D. B., Hart, K. W., Chia, W. N., Barstow, D., Atkinson, T., Munro, I., & Holbrook, J. J. (1987) *Biochim. Biophys. Acta 913*, 66−71.
Willaert, K., Loewenthal., R., Sancho, J., Froeyen, M., Fersht, A., & Engelborghs, Y. (1992) *Biochemistry 31*, 711−716.

BI9603478